The prepower stroke conformation of myosin V

Stan Burgess,[1] Matt Walker,[1] Fei Wang,[2] James R. Sellers,[2] Howard D. White,[3] Peter J. Knight,[1] and John Trinick[1]

[1]Astbury Centre for Structural Molecular Biology and School of Biomedical Sciences, University of Leeds, Leeds, LS2 9JT, UK
[2]Laboratory of Molecular Cardiology, National Heart, Lung and Blood Institute, National Institutes of Health, Bethesda, MD 20892
[3]Department of Physiological Sciences, Eastern Virginia Medical School, Norfolk, VA 23507

We have used electron microscopy and single-particle image processing to study head conformation in myosin V molecules. We find that in the presence of ATP, many heads have a sharply angled conformation that is rare in its absence. The sharply angled conformation is similar to a myosin II atomic structure proposed to mimic the prepower stroke state. The leading head in molecules attached to actin by both heads has a similar conformation, but is also sharply angled in a second plane by tethering through the trail head. The lead head lever joins the motor domain ∼5 nm axially from where it joins the trail motor. These positions locate the converter subdomain and show the lead motor is in the prepower stroke conformation. Tethering by the trail head places the lead head motor domain at the correct axial position along the actin for binding, but at the wrong orientation. Attachment is achieved either by bending the lead head lever throughout its length or at the pliant point. The microscopy shows that most of the walking stride is produced by changes in lever angle brought about by converter movement, but is augmented by distortion produced by thermal energy.

Introduction

The "tilting cross-bridge" hypothesis of force generation by myosin is widely accepted, but remains unproven. In its initial form, the hypothesis proposed that force originates from a change in attachment angle of the myosin head on actin (Huxley, 1969). Subsequent evidence, principally atomic structures of heads, suggested that force results from a conformational change within the head itself. Houdusse et al. (1999, 2000) proposed that the motor domain that binds to actin can be considered as four subdomains linked by three flexible connectors (Fig. 1). The lever is a long α-helical segment extending from the converter subdomain of the motor complexed with light chains. Heads crystallized in different biochemical states reveal little relative movement of three subdomains, but the converter and lever make large, concerted movements with a fulcrum between the so-called SH1 and SH2 helices (Fig. 1). This position has also been inferred from in vitro motility and optical trap experiments where lever length was varied (Uyeda et al., 1996; Ruff et al., 2001). Different converter positions change the lever angle up to ∼80°, which is suggested to be the origin of force (Rayment et al., 1993; Smith and Rayment, 1996; Dominguez et al., 1998; Houdusse et al., 1999, 2000). Although the tilting model of force production is widely accepted, an alternative "thermal ratchet" mechanism has been proposed involving biased Brownian motion of heads along actin (Yanagida et al., 2000). This model has recently received support from considerations of the link between structure and kinetics (Houdusse and Sweeney, 2001), and because of reports of disproportionately large step sizes in myosins with short levers (Nishikawa et al., 2002). Therefore, how myosin moves remains highly controversial.

Force is fuelled by the myosin ATPase (for review see Geeves and Holmes, 1999). The coupling between the enzymic and mechanical steps was first described by Lymn and Taylor (1971) who showed that the low ATPase without actin is due to slow release of the hydrolysis products orthophosphate (Pi)* and ADP. Thus, in steady state, few heads are either empty (apo state) or have only ADP. Hydrolysis is, however, reversible with an equilibrium constant <10; so depending on species and conditions, up to ∼50% of heads have ATP bound rather than ADP and Pi. Binding to actin accelerates product release and force accompanies release of phosphate. A key feature of the Lymn-Taylor scheme is that heads execute the reverse of the power stoke in the detached state on hydrolysis.
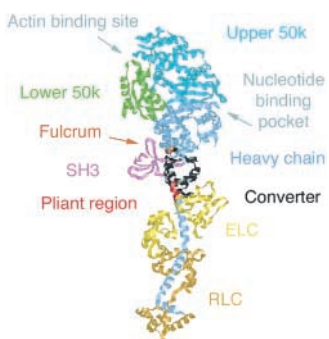
Head crystal structures have been classified into two groups according to whether their levers would be at the start or end of the working stroke if docked onto actin (Geeves

*Abbreviations used in this paper: HMM, heavy meromyosin; Pi, orthophosphate.

Figure 1.   **Crystal structure of the scallop myosin II apoenzyme.** The motor domain is formed by the heavy chain and contains the nucleotide binding pocket and actin binding site. A cleft divides upper and lower 50-kD subdomains, and the SH3 β-barrel of the NH$_2$-terminal subdomain is prominent. The COOH-terminal element of the converter is an α-helix extending into the lever, which is complexed by the essential and regulatory light chains (ELC and RLC, respectively). Between the converter and ELC, a few residues of the heavy chain form a pliant region allowing the lever to bend relative to the motor. The fulcrum for ATP-driven lever movement is within the motor domain (orange spacefilled residue). This and all subsequent atomic diagrams were made using RasMol (Sayle and Milner-White, 1995).

and Holmes, 1999; Houdusse et al., 2000). However, there is evidence from other techniques, such as optical trapping, FRET, ESR and electron microscopy, of multiple stages within the working stroke (Whittaker et al., 1995; Gollub et al., 1999; Veigel et al., 1999; Shih et al., 2000). To avoid the dynamics of hydrolysis, stable complexes with ADP and with ADP plus AlF$_4$, BeF$_x$, or VO$_4$ have generally been crystallized, but interpreting which states of the ATPase these represent has not been straightforward. Structures with ADP.AlF$_4$ or ADP.VO$_4$ are thought to resemble the transition or metastable state of hydrolysis, which may be similar to the conformation with ADP.Pi (Fisher et al., 1995; Dominguez et al., 1998; Houdusse et al., 2000). But there have been conflicting claims as to whether crystallization without nucleotide is representative of rigor or ATP-like states. And structures with ADP.BeF$_x$ present have been found in both start and end conformations. Thus, it is still unclear what shape changes occur as heads progress through the physiological ATPase cycle. Moreover, lever angle is not determined solely by the converter position. Variable bending of the lever at a pliant region where it joins the converter may store cross-bridge energy (Houdusse et al., 2000; Fig. 1). Thus, different lever angles may result both from active converter movements or from passive bending at the pliant region.

Electron microscopy of proteins achieves substantially lower resolution than crystallography, but has the advantages of not requiring a single conformation and being readily applicable to large complexes. Thus, in support of the tilting lever hypothesis, changes in lever angle of ∼30° in attached heads of some types of myosin have been shown on ADP release, reflecting events at the end of the working stroke (Jontes et al., 1995; Whittaker et al., 1995; Volkmann et al., 2000). However, the conformations of attached heads containing ATP or ADP.Pi earlier in the working stroke are more difficult to study. Because of their lower af-

finity ($K_d > 10$ μM), these intermediate states detach from actin at the low protein concentration required for electron microscopy. Lack of information about the start of the working stroke has been the single most important impediment to understanding force production.

All of the crystallography and most of the electron microscopy have used class II myosin heads. However, there are 17 other, so-called unconventional myosin classes (Berg et al., 2001) that may offer advantages for study of force production. Motor domain sequences in these molecules are largely conserved, with differences mainly in surface loops compared with class II myosins (Sellers et al., 1996). Thus, the myosin II head crystal structures are excellent models for unconventional myosins. Single myosin V molecules drag cargoes by walking "processively" along actin filaments without detaching (Mehta et al., 1999; Rief et al., 2000), with heads twice as long as in myosin II, due to six rather than two light chains (Espreafico et al., 1992). This allows the heads in a molecule to span the actin helical repeat and thereby walk straight (Howard, 1997; Vale and Milligan, 2000; Walker et al., 2000). Roles attributed to myosin V include transport of mRNA and vesicles, determination of cell polarity and membrane trafficking (Reck-Peterson et al., 2000).

The myosin V ATPase intermediate states bind to actin more tightly than those of myosin II (de la Cruz et al., 1999; Wang et al., 2000; Yengo et al., 2002), probably to maintain attachment during walking. This allowed us to obtain micrographs of molecules walking along actin during ATP hydrolysis (Walker et al., 2000). When attached by both heads, the lead lever emerged from the motor domain at ∼115° to the actin filament, compared with ∼40° in trail heads at the end of their power stroke. We suggested that the lead head showed for the first time a head in the pre-power stroke conformation on actin. However, no attempt was made to correlate the head shapes with head atomic structures. Since then, new structures (Houdusse et al., 2000) facilitate this comparison.

Here, we report electron microscopy of myosin V heads not attached to actin, without nucleotide and in steady-state ATP hydrolysis. We visualize for the first time a large conformational change between these conditions and compare this with different myosin II head crystal structures. New image averages of lead and trail heads on actin filaments now show the lever clearly resolved. Comparisons with atomic models of heads docked on actin demonstrate that the lead head is at the start of its power stroke. The conformational change in the detached head is the reversal of the power stroke, as postulated by Lymn and Taylor (1971). We show that the majority of the myosin V walking stride results from tilting of the lever. But distortions produced by thermal energy are necessary to attach both heads and, therefore, make a contribution to walking.

Results
Effect of ATP on myosin V HMM
Fig. 2 shows molecules of negatively stained myosin V heavy meromyosin (HMM) with and without ATP. We refer to these datasets as apo and nucleotide heads. Under both conditions, the two heads form an approximate V shape, with
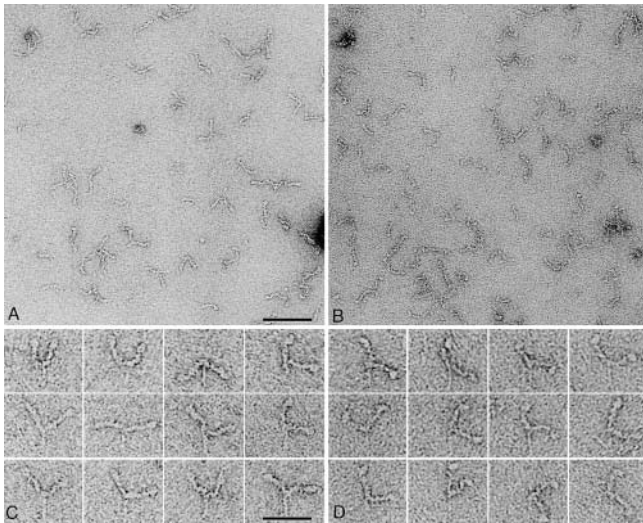
Figure 2. **Negatively stained myosin V HMM molecules.** Fields of molecules in the absence (A) and presence (B) of nucleotide (100 μM ATP; 20°C). Galleries of molecules in the absence (C) and presence (D) of nucleotide. We consistently found image quality to be better without nucleotide. Bars: 100 nm (A and B); 50 nm (C and D).

the motor domain visible as a bulbous tip on each. The lever is segmented, suggestive of the six calmodulin subunits, and is sometimes curved or sharply bent along its length. Frequently, the thinner tail is also visible with the predicted length of 27 nm. Strikingly, many of the nucleotide heads are sharply bent at the motor domain–lever junction. Apo heads are straighter and rarely heavily bent.

Head appearance is variable and obscured by image noise, due mainly to stain variation. To reduce the noise, heads were windowed out and subjected to single-particle image processing using the SPIDER suite of programs (Frank et al., 1996). The number of classes chosen was varied over a

wide range (10–150) to find the best compromise between the need to minimize variability within classes and retain sufficient images in each to benefit from averaging. Fig. 3 shows segregation into 60 classes. These show much more detail than individual images and reveal considerable variability in head appearance. Nucleotide and apo heads are unevenly distributed among the classes. Notably, there are 14 classes where nucleotide heads dominate apo heads by >10-fold (Fig. 3, asterisks), including six with only nucleotide heads. These classes account for 45% of all nucleotide heads, but only 2% of apo heads. Heads in these classes are sharply angled between the lever and motor domain. In contrast, classes dominated by apo heads are less exclusive and not sharply angled. Thus, ATP produces a dramatic change in lever angle. In the sharply angled, mainly nucleotide classes, the motor domains have a protrusion near the junction with the lever. A similar appearance is occasionally seen in mainly apo classes (Fig. 3, black spots), but here the lever angle differs by ∼90°.

Motor domains in mainly nucleotide classes always bend to the right. This shows that myosin V adsorbs to the carbon film in preferred orientations, as does myosin II (Knight and Trinick, 1984; Walker et al., 1985; Burgess et al., 1997). This behavior is also obvious in mainly apo classes, where the motors are smoothly rounded on their right side, with one or two prominent indentations on the left.

Comparison with atomic structures

To understand the effect of ATP on head shape in three dimensions, we compared the class averages with myosin II head crystal structures. Each crystal structure was filtered to 2-nm resolution and projected in 405 views at quasi-equidistant intervals of 5° (Penczek et al., 1994). At this resolution, the motor domains appear similar, but the converter and lever positions differ. Therefore, we initially compared only motor domain features, concentrating on the most populous

Figure 3. **Image averages of myosin V heads in the absence and presence of ATP.** Aligned images from both conditions ($n = 1,172$ in each case) were pooled and classified into 60 classes. Thus, each class has both apo and nucleotide images (where both exist). (top left to bottom right) Classes are presented in order of increasing value of $n_{nucleotide}/(n_{nucleotide}+n_{apo})$. At bottom right in each panel is the total number of images in the class. The histograms show the numbers of apo (left) or nucleotide (right) images in each class. The length of the lever is about half that observed in individual images. The remainder is lost due to variability in position of the COOH-terminal end. Classes in which $n_{nucleotide}/n_{apo} >10$ are marked with an asterisk. Motor domain morphology in these classes is occasionally seen in classes dominated by apo heads (black spots). Arrowheads indicate the cleft between lower and upper 50-kD subdomains, and the arrow (row 3) points to the nucleotide binding pocket. Panels are 25-nm wide.

Figure 4. Comparisons of myosin V heads with myosin II crystal structures. The most populous apo and nucleotide classes were compared with apo (skeletal and scallop) and transition state (scallop–ADP.VO$_4$ and smooth–ADP.AlF$_4$) crystal structures. Only features within motor domains were used for matching (see Results). In each row of A and B, the levers and converter subdomains of the four crystal structures are different, but the rest of the motor domains are very similar and resemble image average motor domains. (A) Apo myosin V motor domains show broadly two appearances (upper 2 and bottom classes) corresponding to two distinct motor orientations (shown in spacefill diagrams of the scallop apo structure in C). Asterisks mark evidence of flexibility at the motor domain–lever junction (see Results). (B) Nucleotide motor domains show broadly one type of appearance, which most closely resembles the scallop–ADP.VO$_4$ structure (D).
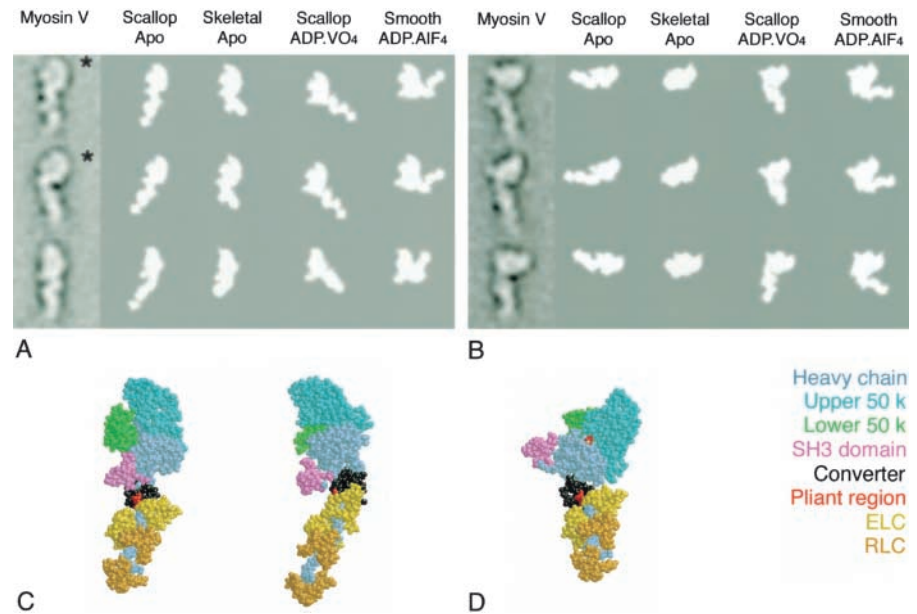

image classes. Fig. 4 shows comparisons of the classes with the most similar projections of two apo and two transition state crystal structures (see Materials and methods). We also made comparisons with the so-called "detached" structure of scallop heads in ADP (Houdusse et al., 1999), but found no orientation of this matching any class.

4 each of the top 12 classes with and without nucleotide were similar to the models in general, but not in every feature. This may be due to shortcomings of negative staining, or because heads adopt conformations not yet crystallized. However, the remaining eight classes, both with and without nucleotide, matched crystal structures strikingly well. From these, three representative examples of each are shown (Fig. 4, A and B).

Apo motor domains have broadly two appearances. Each can be matched by a different crystal structure projection showing it is a different orientation of the same object. The orientations are related by rotation of ∼50° about the motor domain long axis (Fig. 4 C). Lever angles in apo classes are unlike either of the transition state structures, but instead are between the two apo crystal structures (Fig. 4 A).

Motor domains in mainly nucleotide classes have broadly one orientation (Fig. 4 B), which is intermediate between the apo classes (Fig. 4, compare C with D). Lever angles in the nucleotide classes are consistently much like the scallop–ADP.VO$_4$ structure, confirming that the highly bent shape of nucleotide heads originates from a change from an apo-like structure to a scallop–ADP.VO$_4$-like structure. The lever movement induced by this change is large, ∼90°.

Particular image features also can be identified. A distinctive protrusion visible in one orientation of apo heads (Fig. 4 A, top two rows) is the lower 50-kD subdomain (Fig. 4, C and D, red). Immediately above this is an indentation that is the cleft separating the lower and upper 50-kD subdomains. Below the lower 50-kD subdomain is another protrusion corresponding to the SH3 β-barrel (residues ∼30–80). This structure can be seen most clearly in apo heads in the second

orientation (Fig. 4 A, third row, and Fig. 4 C, right) and in nucleotide heads (Fig. 4, B and D). The cleft between the lower and upper 50-kD subdomains can be seen more favorably in other classes (Fig. 3, arrowheads), as can the nucleotide binding pocket (Fig. 3, arrow).

Flexibility in heads

Two apo classes have similar motor domains but different lever angles (Fig. 4 A, asterisks). One is straight (Fig. 4 A, top asterisk), the other angled near the motor–lever junction. In the more angled class, the lever angle is superficially similar to both skeletal-apo and scallop–ADP.VO$_4$ projections. However, the point of emergence of the lever in these crystal structures is different. In the scallop–ADP.VO$_4$ projection, the lever emerges from the lower right of the motor domain, whereas in the skeletal-apo projection, it emerges from the lower left. This results from a change in converter position. In the sharply angled apo class (Fig. 4 A, lower asterisk) the emergence point of the lever most closely resembles the skeletal-apo structure.

In the other class (Fig. 4 A, top asterisk), the head is most like the scallop apo structure in lever angle and point of emergence from the motor. The main difference between the two apo crystal structures is in the lever angle, due to flexibility at the pliant region. The finding that projections of different apo crystal structures match particular apo classes demonstrates flexibility in myosin V at or near the pliant region. Similar behavior was seen in stained rabbit myosin II heads (Burgess et al., 1997). Flexibility between the motor and lever is also suggested in nucleotide-containing heads (Fig. 4 B).

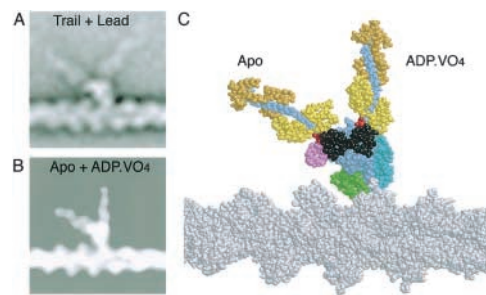## Conformations of myosin V heads attached to actin

We previously presented global lead and trail head image averages of myosin V molecules attached to actin by both heads (Walker et al., 2000). However, these showed blurring of the levers due to variability in position. Some of this variability derives from the fact that heads can attach 11, 13, or
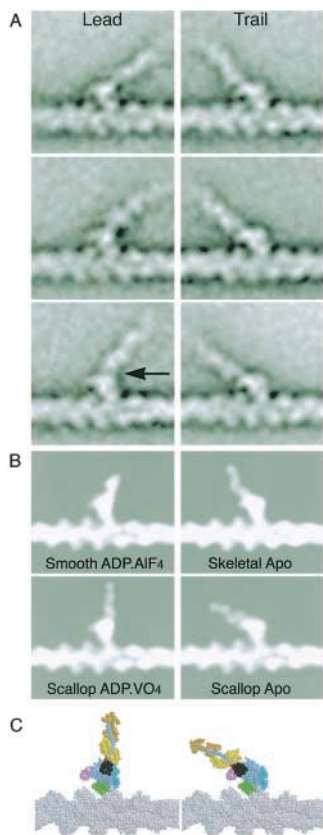
Figure 5. **Comparisons of myosin heads bound to actin with crystal structures of myosin II docked onto actin.** (A) Image averages produced by classifying into six and four classes, respectively, 150 lead and 176 trail heads from molecules attached by both heads. Walking is toward the left in this and the following figures. (B) Models produced by docking head crystal structures with the atomic model of the actin filament (Lorenz et al., 1993) followed by low-pass filtering to 2-nm resolution. Note the similarity in appearance of the actin and myosin with A. (C) Colored models of scallop structures docked onto actin. The arrow marks the pliant point. The angle between the lever arm and the actin filament was 129–143° in lead heads and 39–49° in trail heads. Note also that the sharp bend of the scallop–ADP.VO$_4$ structure is perpendicular to this view and does not show. The converter (black) and lever move in the plane of the page relative to the rest of the motor.

Figure 6. **Demonstration that lead and trail heads have their converters in different positions.** Composite images were produced by superposition of image averages (A) and atomic models of docked scallop apo and ADP.VO$_4$ structures (B and C). Note the points of emergence of the levers (i.e., the pliant regions) differ by ∼5 nm in the image averages (compare with the actin subunit spacing) and 3.6 nm in the atomic models.

15 actin subunits apart (Walker et al., 2000) and some from flexibility within the lever. Lead and trail heads have now been classified into subgroups and averaged, revealing new details of the lever and its point of attachment (Fig. 5 A). At the resolution (∼2 nm) and orientation of these classes, lead and trail motor domains look similar in shape, orientation, and docking geometry and the underlying actin structure appears unchanged. The levers show a segmented appearance suggestive of the calmodulin subunits. A protrusion on the leading side of the motor domain is more prominent in the lead head because it stands alone, whereas in the trail head the lever is nearby.

The principal difference between subgroups is the lever angle, with bending at or near the pliant region. Although some lead head levers are curved in the raw data, the lever classes are largely straight. The absence of strongly curved classes suggests that the curved levers are heterogeneous. All the sub-groups show clearly that the lead head lever emerges from the motor domain near its trailing edge, whereas the trail head lever emerges from its front (Fig. 5 A). The difference between the points of emergence is large, ∼5 nm. Few if any lead heads in the raw images, including those with curved levers, show features compatible with the lever emerging from the front of the motor domain.

Comparison with docked atomic structures

The lead and trail head classes were compared with atomic models. These were created from the four head crystal structures used above docked onto actin with a constant motor attachment geometry (Fig. 5, B and C; see Materials and methods). In projection, the appearance of the actin filament is sensitive to small changes in azimuth, so we were able to choose an orientation best matching the classes. Fig. 5 B has grayscale panels for comparison with the image averages. Fig. 5 C shows colored spacefill models to facilitate identification of different regions.

In most respects, the similarity of the models to our data is very strong, although the contacts of the motor with the actin appear more extensive than in the model. The lead and trail motor domains resemble one another and the docked model motors. This confirms that the orientation of the lead motor is similar to rigor and that the protrusion on its leading side is the SH3 β-barrel (Fig. 5 C). The angle of trail head levers varies by ∼20°, but the orientation shown in the right panels of Fig. 5 A is similar to the docked scallop apo model. Strikingly, however, the lead head levers are unlike either of the docked transition state structures in being bent backward along the filament by 40–55°. By comparison, the docked smooth–ADP.AlF$_4$ lever is bent backward by 30° in this view and scallop–ADP.VO$_4$ lever is perpendicular to the actin filament.

Fig. 6 A shows lead and trail head subclasses superimposed at the motor domain. This demonstrates separation of the lead and trail levers that, because of their widely different points of attachment to the motor, do not coincide anywhere along their length. The superimposed scallop apo and transition state crystal structures show just the same feature (Fig. 6 B). The spacefill diagram of the superimposed models (Fig. 6 C) makes it clear that the reason the

apo and transition state levers do not coincide is that their converters (black) are in very different positions, such that points at which the levers emerge (the pliant region) are 3.6 nm apart. Thus, the lever acts as a marker of converter position and shows that in lead head images it is in a position similar to that in the docked scallop–ADP.VO$_4$ and smooth–ADP.AlF$_4$ crystal structures. Indeed the leading part of the trail motor behind the SH3 domain is more prominent because the converter has moved there. The lead head appearance could not possibly be reproduced by bending the apo crystal structure lever backward at the pliant region (Fig. 6 C). These comparisons show that the motor domain of the lead head shares key similarities with the atomic structures thought to precede the working stroke, and has not progressed to the rigor conformation.

Discussion

X-ray crystallography has been crucial in providing atomic descriptions of myosin II heads and the actin monomer, and in providing the basis for describing how force may be generated within the head. However, crystallization is incompatible with gross conformational changes during a catalytic cycle, necessitating the use of long-lived analogues such as ADP.VO$_4$ and ADP.AlF$_4$. Assigning the different analogue structures to particular points in the ATPase cycle has been problematic. By contrast, electron microscopy allows observation of proteins going through their catalytic cycle, using the natural substrate and in complexes that do not crystallize, such as heads on actin. Negative staining has the potential to induce artifacts, but the excellent correspondence between the images described here and the atomic models suggests that the images provide a faithful representation. Although the resolution attainable is lower, ~2 nm here, this is quite sufficient to reveal large changes in conformation such as movements of the lever.

Shape changes in unattached myosin heads

We find that in ATP a strongly angled conformation of the head is produced not seen without ATP, either in the myosin V studied here or myosin II (Burgess et al., 1997). Such heads are likely to be in the ADP.Pi state. However, not all nucleotide heads are strongly angled and about half are in classes with apo heads. A likely explanation for this is that both myosin.ATP and ADP.Pi biochemical states are populated in the steady state. The proportion of molecules in the ADP.Pi state in the myosin V construct we have used is typically ~55% (unpublished data) which is in reasonable agreement with the fraction of highly bent molecules. However, it should be noted that an exact correspondence is not necessarily to be expected because there is evidence from myosin II suggesting that the structural and biochemical states may not be exactly coupled (Malnasi-Csizmadia et al., 2000; Urbanke and Wray, 2001).

Head crystal structures with ATP and its analogues commonly give a structure very similar to apo heads (Fisher et al., 1995; Gulick et al., 1997; Bauer et al., 2000). This suggests that heads bearing ATP would classify together with apo heads, and thus provides an explanation of the many classes with both apo and nucleotide heads, which resemble projections of the scallop apo structure. We found a range of ratios of apo to nucleotide heads in these classes, which may indicate that ATP heads are subtly different from apo heads.

The new data are thus consistent with the idea that the shape of heads in the state that binds to actin at the start of the power stroke is markedly different from that at the end of the stroke, as is required by the tilting lever hypothesis. The similarity of the scallop–ADP.VO$_4$ structure to our images supports the proposal that it represents a prepower stroke conformation.

Shape changes in heads attached to actin

The new actin-attached head classes show greatly improved detail, allowing new conclusions about the state of the lead head. The classes show that the points where the lever joins the motor in lead and trail heads are separated by a large distance, 5 nm. Thus, the converters, though not directly visible, are also in different positions. The models of myosin II heads docked onto actin are entirely compatible with this. Significantly, the models also show a 3.6-nm axial translation of the point of attachment of the lever to the motor (i.e., pliant region). The agreement between this feature of lead and trail heads and their corresponding models precludes an alternative interpretation that the lead head converter is in the apo postpower stroke conformation, with the lever bent backward at the pliant region by strain from the trail head. Therefore, it is clear that the lead head converter is in a grossly different position from that in the trail head and is similar to its position in strongly angled unattached heads. We conclude that the lead head is at the start of its power stroke.

The demonstrations that similar gross conformational changes occur in heads both on and off actin during their ATPase cycle, and that the lead and trail motor domains have similar docking geometry, are compatible with the idea that force production is an intrinsic property of myosin and that the primary mechanical function of actin is to provide the anchorage for force production.

Structural basis of processive movement

Comparisons between the detached, sharply angled, ADP.Pi head and the lead head on actin show different lever angles. The angled shape of the detached head seen in the presence of nucleotide most closely resembles the scallop–ADP.VO$_4$ structure. However, the orientation of the lead head lever is unlike either of the docked transition state structures in being markedly bent backward along the actin filament. It seems likely that the additional bending occurs at the pliant region due to tethering through the trail head.

Bending in the pliant region and throughout the lever may be features of long myosin V strides. During processive movement, the working stroke carries the detached head away from its previous attachment site toward the next (Fig. 7). Images of singly attached molecules indicate that at the end of the working stroke, the lever is at ~40° to the filament axis (Walker et al., 2000) and if ADP is still bound, then the angle is ~50° (Veigel et al., 2002). Either angle is sufficient to position the detached motor adjacent to a binding site 36 nm along the filament (Fig. 7 A). However, even in the sharply angled ADP.Pi conformation (Fig. 7 B), the motor domain orientation is still incorrect for stereospecific binding, though
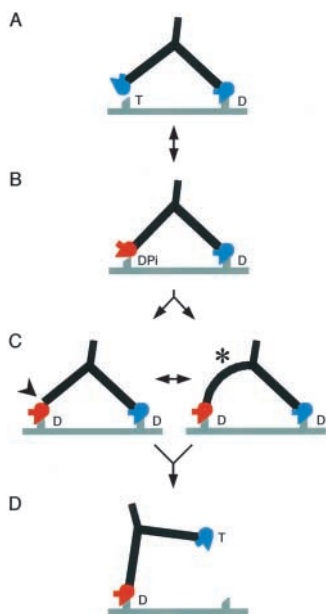
Figure 7. **Structural cycle of myosin V walking.** Red motor domains represent the converter and lever in the prepower stroke conformation, and blue ones represent the postpower stroke conformation. The actin filament is gray and shows two preferred attachment sites for heads spaced by 36 nm. Myosin (drawn to a similar scale) is walking left and has a head orientation that shows a prominent SH3 domain. T, DPi, and D (ATP, ADP + phosphate, and ADP) indicate the likely head nucleotide contents in vivo. Note that if ATP is limiting in vitro, as in our data with actin, then the head contents will be different (see Discussion). (A) The attached head is close to the rigor orientation; the motor domain of the second head can reach the next binding site on actin, but the apo-like head shape is wrong for attachment. (B) The detached head has switched to the angled conformation seen in unattached molecules (Fig. 4 B), which in this view appears straight (Fig. 5 B, scallop–ADP.VO$_4$). The motor domain may attach weakly to actin, but is not oriented correctly for strong binding because the lever is not perpendicular to the actin filament. (C) Stereospecific attachment of the lead head motor to actin. We propose that attachment is achieved by distortion either at the lead head pliant region (arrowhead), or throughout its lever (asterisk). This explains why both straight and curved levers can be seen in lead head images, even though the converters are in the prepower stroke position. Note that little forward movement of the myosin tail accompanies attachment of the lead head. For simplicity, the subsequent actin-activated release of Pi is not shown as a separate step. Note also that though both heads contain only ADP, they have very different conformations. (D) Release of the trail head on binding ATP. The intramolecular strain is relieved, the lead lever becomes nearly perpendicular to the filament and the myosin tail moves forward. This would quickly be followed by the working stroke of the lead head, completing the cycle.

weak binding may be possible (de la Cruz et al., 2001). Attachment could be accomplished in two ways. First, there could be bending throughout the lever such that it joins the motor domain perpendicular to the filament (Fig. 7 C, right), which would allow attachment similar to the docked scallop–ADP.VO$_4$ structure. This would be consistent with the bends seen in detached molecule levers, and with the curved levers in individual lead heads. Alternatively the pliant region could bend, allowing the motor to adopt the correct orientation on an uncurved lever (Fig. 7 C, left). Once attached, these two

distortions could be in dynamic balance, yielding the mixture of curved and straight lead levers we observe (Fig. 7 C). Note that on this view, attachment of the lead head produces little movement of the tail. We envisage that stereospecific binding allows actin to catalyze Pi release.

There are two consequences of these distortions. First, the force required to produce them will not be simply related to the amount of distortion. Once the pliant helix ruptures, it will approximate a freely jointed chain. The energy stored is that required to disrupt the helix. This is different from an elastic diffusive mechanism where greater reach requires progressively greater force (Veigel et al., 2002). Second, when the trail head detaches, refolding of the pliant helix or straightening of the lever will itself produce a forward movement of the cargo along the actin filament (Fig. 7 D). We previously pointed out that the working stroke of the lever appeared to be substantially less than the 36-nm stride length necessary for processive walking (Walker et al., 2000) and optical trap data are consistent with this (Moore et al., 2001; Veigel et al., 2002). Thus, the distortion required to take strides along actin that substantially exceed the working stroke may not show as an extra movement of the tail *following* the working stroke, but may coincide with it or even precede it.

Implications for the structural mechanism of force production

The large changes we see in lever angle in heads attached to actin show that forward motion is produced in large part by a tilting mechanism. We have also now shown that reversal of this conformational change occurs in heads detached from actin, as predicted by the Lymn and Taylor (1971) scheme. However, the micrographs reveal that extra bending in the lead head lever is necessary to allow it to reach out to attach 36 or 41 nm ahead of the trail head, and there may be bending in the trail head too. Thus, tilting alone does not account for all of the translation achieved in a walking stride. The extra reach is facilitated by bending of the lead head at its pliant region, or throughout its lever, and distorts the doubly attached molecule. This distortion is likely to be important in the walking mechanism, allowing strain-dependent steps in the ATPase cycle, possibly ADP release or ATP binding that are important for enhancing processivity. The extra reach must be achieved by diffusion and is thus directed Brownian motion. However, since it appears to be required for the lead head to locate an actin subunit with the correct orientation, this thermally induced motion is not the type of diffusive mechanism proposed by Yanagida and coworkers, where heads are proposed to glide between subunits.

Our result that the lead head converter is in the prepower stroke position bears on the mechanism of force production by the myosin superfamily. In a two-headed processive myosin, it has not been established how far the lead head progresses through product release states before the trail head detaches. Converter movement is generally thought to precede Pi release (Geeves and Holmes, 1999) because conversion of the motor to the postpower stroke structure is thought to accompany tight binding to actin, and this should precede product release. Moreover, an attractive mechanism to enhance processivity is for product release from the lead head to be gated to movement of the lever by

the tether through the trail head. In such a mechanism, the lead head would retain both products until the trail head detaches from actin when ATP binds (de la Cruz et al., 2001; Veigel et al., 2002). In the presence of 1 μM ATP, as used here, the stepping rate is ~1 s^{-1}, so the lead heads in our images will have been in that position for 0.7 s on average. However, for 90% of the products to remain, their rates of release would have to be reduced by ~2,500-fold (Pi) and ~120-fold (ADP) compared with those measured in single, unconstrained heads (~250 and 12 s^{-1}, respectively for acto–myosin V subfragment 1; de la Cruz et al., 1999).

The alternative possibility is that the lead head has lost one or both hydrolysis products, but its converter is constrained from moving to the post power stroke position by being tethered through the trail head. Thus, product release may precede, rather than follow converter movement. Actin, whose mode of activation of product release from the motor domain is unknown at the atomic level, may thus become tightly bound to the motor and stimulate product release, without converter movement. This would be logical because the head would then exert force only after tight binding rather than before. Pi release is by a "back door" (Yount et al., 1995) cleft that is thought to narrow on tight binding to actin. Therefore, it has generally been assumed that release would be blocked after tight binding and that Pi must therefore detach first (Houdusse and Sweeney, 2001), but this may not be the case on actin. ADP could be released soon after Pi or retained until the trail head detaches when it binds ATP. Retention would prevent futile cycles of ATP binding by the lead head.

How could the trail head tether stop the lead head converter moving to the postpower stroke position? Inspection of the apo head docked on actin (Fig. 5 C) suggests that steric hindrance between the first light chain and the motor domain would prevent the lever bending backward at the pliant region. Thus, forward movement of the converter would require major distortion of the lever itself, which we do not find. Such steric hindrance would not occur in the docked ADP.VO$_4$ head structure because the converter is in a different position and the lever would not collide with the motor domain on bending backward. When actin induces changes that favor a postpower stroke position of the converter, the motor domain must become internally stressed and thus exert a force between the converter and actin. This mechanism differs from the proposal of Houdusse and Sweeney (2001) that converter movement precedes Pi release resulting in distortion of the lever. Steric inhibition of converter movement and consequent storage of stress within the motor domain could be a mechanism for force generation common to all myosins.

Materials and methods

Proteins

Mouse myosin V HMM (residues 1–1,091; provided by John Hammer, III, National Institutes of Health) and calmodulin were expressed in Sf9 cells by coinfection with baculovirus vectors, purified as described previously (Wang et al., 2000) to a concentration of ~1 μM in 0.5 M KCl, 0.1 mM EGTA, 1 mM DTT, and 10 mM MOPS, pH 7.0. Rabbit skeletal muscle G-actin in 0.2 mM CaCl$_2$, 0.5 mM DTT, 0.2 mM ATP, and 2 mM Tris-HCl, pH 8.0, was polymerized by addition of 0.2 mM EGTA, 0.1 mM MgCl$_2$, followed after 15 min by 50 mM KCl. Both HMM and G-actin were stored by dropwise freezing in liquid nitrogen.

Electron microscopy

Thawed proteins were diluted in 100 mM KCl, 0.1 mM EGTA, 1 mM MgCl$_2$, and 10 mM MOPS, pH 7.0, applied to grids with a thin carbon film, and negatively stained with 1% uranyl acetate as described by Walker et al. (1985), but without a buffer rinse before staining. Final protein concentrations were 40 nM HMM or 1 μM actin plus 80 nM HMM. Micrographs were recorded on a JEOL 1200ex microscope at moderate dose (~100 e/Å^2), digitized at a step-size corresponding to 0.53 nm and imported into the SPIDER software suite.

Image processing

Individual heads were windowed out in micrographs. From 29 micrographs of molecules in the presence of ATP and 25 micrographs in its absence a total of 3,064 ATP heads and 2,955 apo heads were selected, pooled, and aligned by reference-free methods. We tested a variety of classification methods and, as with our previous work on myosin II (Burgess et al., 1997), we found that "K-means clustering" (Frank, 1996) was most useful. An initial classification into 200 classes was used to eliminate heads that were misaligned or poorly stained. From those remaining, 2,344 images (1,172 from each nucleotide state) were subjected to a second round of classification. Due to evidence of flexibility within the lever (Fig. 2), classification used a mask including only the motor domain and the first part of the lever.

Alignment of myosins attached to actin by both heads has been described briefly (Walker et al., 2000). Identifying lead and trail heads among the two-headed molecules requires determination of actin filament polarity. For this, we developed a novel filament alignment strategy using single-particle methods. Filaments were computationally divided into short segments, 15 subunits long (sufficient to span the longest expected helical repeat) and aligned by a novel single-particle reference–based algorithm. The starting reference image was generated from a model of a continuous helix having a diameter and pitch similar to F-actin, although these values were not critical. The global average of aligned segments after each round of alignment was used as the reference in the next iteration. During alignment rotation angles (±180°) were constrained so that all segments from a filament had the same polarity.

Having aligned the actin segment to which each individual head was attached, the alignment was refined to bring the motors into translational registration. This was achieved by windowing out only the motor portion of the image (excluding actin and the lever). Reference-based alignment was performed iteratively, using the cross-correlation function against the current global average. Individual images of heads bound to actin were then segregated into lead and trail groups and translational refinement was repeated. Images were classified by hierarchical ascendant classification after correspondence analysis (Frank, 1996), using a mask that contained only the levers.

Crystal structures

The crystal structures of two apoenzymes of myosin II subfragment 1 were used: (1) from chicken skeletal muscle (accession no. 2mys [Rayment et al., 1993]; referred to here as skeletal apo) and (2) from scallop muscle (accession no. 1dfk [Houdusse et al., 2000]; scallop apo). Two transition state structures of myosin II were also used: from scallop muscle with ADP and VO$_4$ bound (accession no. 1dfl [Houdusse et al., 2000]; scallop–ADP.VO$_4$), and smooth muscle with ADP and AlF$_4$ bound (accession no. 1br1 [Dominguez et al., 1998]; smooth–ADP.AlF$_4$). A model of the smooth–ADP.AlF$_4$ structure containing a regulatory light chain was constructed using chains A and B of 1br1 and the regulatory domain of scallop, accession no. 1wdc (Houdusse and Cohen, 1996). The regulatory light chain and the sequence of the heavy chain running through it were docked onto 1br1 by aligning the IQ sequences in the essential light chains (785–795 in 1wdc and 799–809 in 1br1) using Deep View (Guex and Peitsch, 1997).

Docking the motor domain of head crystal structures onto actin used a model of F-actin (Lorenz et al., 1993) and the docking geometry of the chicken apoenzyme as described (accession no. 1alm) by Mendelson and Morris (1997). Regions of the motor domains of other head structures were superimposed on the chicken structure using Deep View. The position of the motor domain on actin in this model was assumed to be invariant with nucleotide content between residues homologous to G466-E476 and S534-K598 in the chicken skeletal sequence and these sequences are highly conserved. At the orientation and resolution of our data, the differences between this docking and others were imperceptible.

Rayment for the complete coordinates of the chicken skeletal head, and Ed Morris for docking the chicken structure with sidechains onto actin.

References

Bauer, C.B., H.M. Holden, J.B. Thoden, R. Smith, and I. Rayment. 2000. X-ray structures of the apo and MgATP-bound states of *Dictyostelium discoideum* myosin motor domain. *J. Biol. Chem.* 275:38494–38499.

Berg, J.S., B.C. Powell, and R.E. Cheney. 2001. A millennial myosin census. *Mol. Biol. Cell.* 12:780–794.

Burgess, S.A., M. Walker, H.D. White, and J. Trinick. 1997. Flexibility within myosin heads revealed by negative stain and single-particle analysis. *J. Cell Biol.* 139:675–681.

de la Cruz, E.M., A.L. Wells, S.S. Rosenfeld, E.M. Ostap, and H.L. Sweeney. 1999. The kinetic mechanism of myosin V. *Proc. Natl. Acad. Sci. USA.* 96:13726–13731.

de la Cruz, E.M., E.M. Ostap, and H.L. Sweeney. 2001. Kinetic mechanism and regulation of myosin VI. *J. Biol. Chem.* 276:32373–32381.

Dominguez, R., Y. Freyzon, K.M. Trybus, and C. Cohen. 1998. Crystal structure of a vertebrate smooth muscle myosin motor domain and its complex with the essential light chain: visualization of the pre-power stroke state. *Cell.* 94:559–571.

Espreafico, E.M., R.E. Cheney, M. Matteoli, A.A.C. Nascimento, P.V. Decamilli, R.E. Larson, and M.S. Mooseker. 1992. Primary structure and cellular-localization of chicken brain myosin-V P190, an unconventional myosin with calmodulin light-chains. *J. Cell Biol.* 119:1541–1557.

Fisher, A.J., C.A. Smith, J.B. Thoden, R. Smith, K. Sutoh, H.M. Holden, and I. Rayment. 1995. X-ray structures of the myosin motor domain of *Dictyostelium discoideum* complexed with MgADP.BeF$_x$ and MgADP.AlF$_4$. *Biochemistry.* 34:8960–8972.

Frank, J. 1996. Three-dimensional Electron Microscopy of Macromolecular Assemblies. Academic Press Inc., San Diego. 342 pp.

Frank, J., M. Radermacher, P. Penczek, J. Zhu, Y.H. Li, M. Ladjadj, and A. Leith. 1996. Spider and web-processing and visualization of images in 3D electron-microscopy and related fields. *J. Struct. Biol.* 116:190–199.

Geeves, M.A., and K.C. Holmes. 1999. Structural mechanism of muscle contraction. *Annu. Rev. Biochem.* 68:687–728.

Gollub, J., C.R. Cremo, and R. Cooke. 1999. Phosphorylation regulates the ADP-induced rotation of the light chain domain of smooth muscle myosin. *Biochemistry.* 38:10107–10118.

Guex, N., and M.C. Peitsch. 1997. SWISS-MODEL and the Swiss-PdbViewer: an environment for comparative protein modeling. *Electrophoresis.* 18:2714–2723.

Gulick, A.M., C.B. Bauer, J.B. Thoden, and I. Rayment. 1997. X-ray structures of the MgADP, MgATP gamma S, and MgAMPPNP complexes of the *Dictyostelium discoideum* myosin motor domain. *Biochemistry.* 36:11619–11628.

Houdusse, A., and C. Cohen. 1996. Structure of the regulatory domain of scallop myosin at 2-angstrom resolution: implications for regulation. *Structure.* 4:21–32.

Houdusse, A., V.N. Kalbokis, D. Himmel, A.G. Szent-Györgyi, and C. Cohen. 1999. Atomic structure of scallop myosin subfragment S1 complexed with MgADP: a novel conformation of the myosin head. *Cell.* 97:459–470.

Houdusse, A., and H.L. Sweeney. 2001. Myosin motors: missing structures and hidden springs. *Curr. Opin. Struct. Biol.* 11:182–194.

Houdusse, A., A.G. Szent-Györgyi, and C. Cohen. 2000. Three conformational states of scallop myosin S1. *Proc. Natl. Acad. Sci. USA.* 97:11238–11243.

Howard, J. 1997. Molecular motors: structural adaptations to cellular functions. *Nature.* 389:561–567.

Huxley, H.E. 1969. The mechanism of muscle contraction. *Science.* 164:1356–1366.

Jontes, J.D., E.M. Wilson-Kubalek, and R.A. Milligan. 1995. A 32-degree tail swing in brush-border myosin-I on ADP release. *Nature.* 378:751–753.

Knight, P., and J. Trinick. 1984. Structure of the myosin projections on native thick filaments from vertebrate skeletal-muscle. *J. Mol. Biol.* 177:461–482.

Lorenz, M., D. Popp, and K.C. Holmes. 1993. Refinement of the F-actin model against X-ray fiber diffraction data by the use of a directed mutation algorithm. *J. Mol. Biol.* 234:826–836.

Lymn, R.W., and E.W. Taylor. 1971. Mechanism of adenosine triphosphate hydrolysis of acto-myosin. *Biochemistry.* 10:4617–4624.

Malnasi-Csizmadia, A., R.J. Woolley, and C.R. Bagshaw. 2000. Resolution of conformational states of *Dictyostelium* myosin II motor domain using tryptophan W501 mutants: implications for the open-closed transition identified by crystallography. *Biochemistry.* 39:16135–16146.

Mehta, A.D., R.S. Rock, M. Rief, J.A. Spudich, M.S. Mooseker, and R.E. Cheney. 1999. Myosin-V is a processive actin-based motor. *Nature.* 400:590–593.

Mendelson, R., and E.P. Morris. 1997. The structure of the acto-myosin subfragment 1 complex: results of searches using data from electron microscopy and x-ray crystallography. *Proc. Natl. Acad. Sci. USA.* 94:8533–8538.

Moore, J.R., E.B. Krementsova, K.M. Trybus, and D.M. Warshaw. 2001. Myosin V exhibits a high duty cycle and large unitary displacement. *J. Cell Biol.* 155:625–635.

Nishikawa, S., K. Homma, Y. Komori, M. Iwaki, T. Wazawa, A.H. Iwane, J. Saito, R. Ikebe, E. Katayama, T. Yanagida, and M. Ikebe. 2002. Class VI myosin moves processively along actin filaments backward with large steps. *Biochem. Biophys. Res. Commun.* 290:311–317.

Penczek, P.A., R.A. Grassucci, and J. Frank. 1994. The ribosome at improved resolution: new techniques for merging and orientation refinement in 3D cryo-electron microscopy of biological particles. *Ultramicroscopy.* 53:251–270.

Rayment, I., W.R. Rypniewski, K. Schmidtbase, R. Smith, D.R. Tomchick, M.M. Benning, D.A. Winkelmann, G. Wesenberg, and H.M. Holden. 1993. Three-dimensional structure of myosin subfragment-1: a molecular motor. *Science.* 261:50–58.

Reck-Peterson, S.L., D.W. Provance, Jr., M.S. Mooseker, and J.A. Mercer. 2000. Class V myosins. *Biochim. Biophys. Acta.* 1496:36–51.

Rief, M., R.S. Rock, A.D. Mehta, M.S. Mooseker, R.E. Cheney, and J.A. Spudich. 2000. Myosin-V stepping kinetics: a molecular model for processivity. *Proc. Natl. Acad. Sci. USA.* 97:9482–9486.

Ruff, C., M. Furch, B. Brenner, D.J. Manstein, and E. Meyhofer. 2001. Single-molecule tracking of myosins with genetically engineered amplifier domains. *Nat. Struct. Biol.* 8:226–229.

Sayle, R., and E.J. Milner-White. 1995. RasMol: biomolecular graphics for all. *Trends Biochem. Sci.* 20:374–376.

Sellers, J.R., H.V. Goodson, and F. Wang. 1996. A myosin family reunion. *J. Muscle Res Cell Motil.* 17:7–22.

Shih, W.M., Z. Gryczynski, J.R. Lakowicz, and J.A. Spudich. 2000. A FRET-based sensor reveals large ATP hydrolysis-induced conformational changes and three distinct states of the molecular motor myosin. *Cell.* 102:683–694.

Smith, C.A., and I. Rayment. 1996. X-ray structure of the magnesiumII.ADP.vanadate complex of the *Dictyostelium discoideum* myosin motor domain to 1.9 Angstrom resolution. *Biochemistry.* 35:5404–5417.

Urbanke, C., and J. Wray. 2001. A fluorescence temperature-jump study of conformational transitions in myosin subfragment 1. *Biochem. J.* 358:165–173.

Uyeda, T.Q.P., P.D. Abramson, and J.A. Spudich. 1996. The neck region of the myosin motor domain acts as a arm to generate movement. *Proc. Natl. Acad. Sci. USA.* 93:4459–4464.

Vale, R.D., and R.A. Milligan. 2000. The way things move: looking under the hood of molecular motor proteins. *Science.* 288:88–95.

Veigel, C., L.M. Coluccio, J.D. Jontes, J.C. Sparrow, R.A. Milligan, and J.E. Molloy. 1999. The motor protein myosin-I produces its working stroke in two steps. *Nature.* 398:530–533.

Veigel, C., F. Wang, M.L. Bartoo, J.A. Sellers, and J.E. Molloy. 2002. The gated gait of the processive molecular motor, myosin V. *Nat. Cell Biol.* 4:59–65.

Volkmann, N., D. Hanein, G. Ouyang, K.M. Trybus, D.J. DeRosier, and S. Lowey. 2000. Evidence for cleft closure in actomyosin upon ADP release. *Nat. Struct. Biol.* 7:1147–1155.

Walker, M., P. Knight, and J. Trinick. 1985. Negative staining of myosin molecules. *J. Mol. Biol.* 184:535–542.

Walker, M.L., S.A. Burgess, J.R. Sellers, F. Wang, J.A. Hammer, III, J. Trinick, and P.J. Knight. 2000. Two-headed binding of a processive myosin to F-actin. *Nature.* 405:804–807.

Wang, F., L.F. Chen, O. Arcucci, E.V. Harvey, B. Bowers, Y.H. Xu, J.A. Hammer, and J.R. Sellers. 2000. Effect of ADP and ionic strength on the kinetic and motile properties of recombinant mouse myosin V. *J. Biol. Chem.* 275:4329–4335.

Whittaker, M., E.M. Wilson-Kubalek, J.E. Smith, L. Faust, R.A. Milligan, and H.L. Sweeney. 1995. A 35-Angstrom movement of smooth-muscle myosin on ADP release. *Nature.* 378:748–751.

Yanagida, T., K. Kitamura, H. Tanaka, A.H. Iwane, and S. Esaki. 2000. Single molecule analysis of the actomyosin motor. *Curr. Opin. Cell Biol.* 12:20–25.

Yengo, C.M., E.M. de la Cruz, D. Safer, E.M. Ostap, and H.L. Sweeney. 2002. Kinetic characterization of the weak binding states of myosin V. *Biochemistry.* 41:8508–8517.

Yount, R.G., D. Lawson, and I. Rayment. 1995. Is myosin a back door enzyme. *Biophys. J.* 68:44S–49S.